

A Compact Wall-Climbing and Surface Adaptation Robot for Non-Destructive Testing

Hernando Leon-Rodriguez^{1*}, Salman Hussain and Tariq Sattar²

¹ Department of Industrial Engineering, Nueva Granada Military University, Bogota, Colombia
(Tel : +57-1-6500-000; E-mail: hernando.leon@unimilitar.edu.co) * Corresponding author

² Department of Engineering and Design, London South Bank University, London, SE1 0AA, England
(Tel : +44-020-7815-7051; E-mail: hussas20@lsbu.ac.uk, sattatp@lsbu.ac.uk)

Abstract: This paper describes the design of an umbilical-free mobile non-destructive testing (NDT) climbing robot for industrial applications that is capable of inspecting oil tanks, pipelines, petro-chemical tanks, bridges, railways, etc. The mechanical design is based on a wheeled mobile robot with magnetic adhesion forces optimised with flux concentrators. The robot carries a NDT wheel probe in order to detect weld defects, wall thickness and corrosion. The robot adapts to surface curvatures (both convex and concave and both along its length and width) and can make transitions between surfaces that have an angle of up to ninety degrees between them. The robot and an on-board NDT Flaw Detector are controlled remotely via wireless communication. Higher level commands remotely adjust NDT parameters, robot speeds, and control inspection tasks from the ground.

Keywords: Non Destructive Testing, Climbing robot, welds defects and corrosion detection.

1. INTRODUCTION

Application areas for automated and robotic non-destructive testing (NDT) are in the inspection of critical infrastructure on offshore oil platforms, nuclear power plant, shipyards, petrochemical and other storage tanks, aircraft, buildings, pipelines, bridges and railways [1, 2, 3]. Access to test sites on these structures is obtained by constructing scaffolding or abseiling down from the top. Erecting scaffolding is expensive and hence testing the structural integrity of these structures is an expensive and time consuming activity. The use of all climbing robots (that are able to deploy NDT sensors) can speed up the inspection, eliminate scaffolding costs and provide access to large structures in hazardous environments which may not be accessible to human inspectors. Inspection of these structures requires that the robots should be able to climb on vertical surfaces, make transitions between surfaces, operate in liquids, deploy a range of NDT sensors with sufficient precision to detect and size defects, acquire defect data and make it available to an NDT inspector for analysis, and be intrinsically safe when operating in explosive and flammable environments.

An increasing interest in the development of special climbing robots has been seen in recent years [5]. This has been motivated by a desire to increase operation efficiency in the performance of dangerous and hazardous tasks by reducing the turn-around time in both planned and unplanned outages. These capabilities in climbing robots would not only allow them to replace human workers in the carrying out of these dangerous duties but would also eliminate costly scaffolding. One of the most interesting applications of a climbing robot involves steel tank inspection. For example, thousands of storage tanks in oil refineries have to be inspected manually to prevent leakage or any other potential catastrophe.

The most important consideration for a climbing robot is its mechanical design; a further important issue

is the implementation of the navigation system. The complexity of finding the robot's location in oil tanks means that most climbing robots are semiautonomous or remote controlled systems [3, 5, 6]. Currently, a climbing autonomous robot uses a surface coverage algorithm based on distance transform function to allow it to navigate itself over the tank surface in a back and forth motion to scan the external wall for possible faults using sensors without any human intervention. The drawback of this autonomous robot is the impossibility of developing inspections based on specific tank areas because the robot's position is not estimated.

A prototype NDT robot is described in this paper which uses permanent magnets, with an air gap of 5 mm to avoid studs, small obstacles, full contact with the surface, etc. The robot is able to attach itself to ferrous surfaces such as ship hulls, box girders, bridges, etc. It is able to change surfaces while maintaining an adhesion force and climb on vertical surfaces. The robot is designed to scan long weld lines with continuous motion. It deploys a dry contact ultrasonic wheel probe to detect weld defects and corrosion in the wall. The ultrasound detector is carried on board the robot; it is completely umbilical free with all control and NDT data acquisition on-board and controlled wirelessly using WiFi technology. The NDT inspector is able to control the robot via a PC laptop computer and set all parameters from the ground. The robot saves all data on-board, so in case of loss of communication with the ground, it keeps on collecting data until the communication is restored.

The robot can make a transition between two surfaces at a maximum angle of 60 degrees. It can cope with surface curvatures with a minimum diameter of 1 metre. It can be attached to the surface from inside or outside and inspect for defects. Its mass is 5 kg which makes its deployment very easy and since it performs the inspection wirelessly there are no umbilical management problems. The payload consists of an ultrasound USB-NDT card, a small computer, an

ultrasound wheel probe for NDT, batteries and motor control cards.

2. DESIGN OF THE ULTRASOUND NDT ROBOT

The NDT robot is designed and built, shown in Figure 1, to have three hinged sections, with three groups of wheels to drive the robot, and one support wheel in the front. The two sets of wheels in each half of the robot are driven differentially by four DC motors.

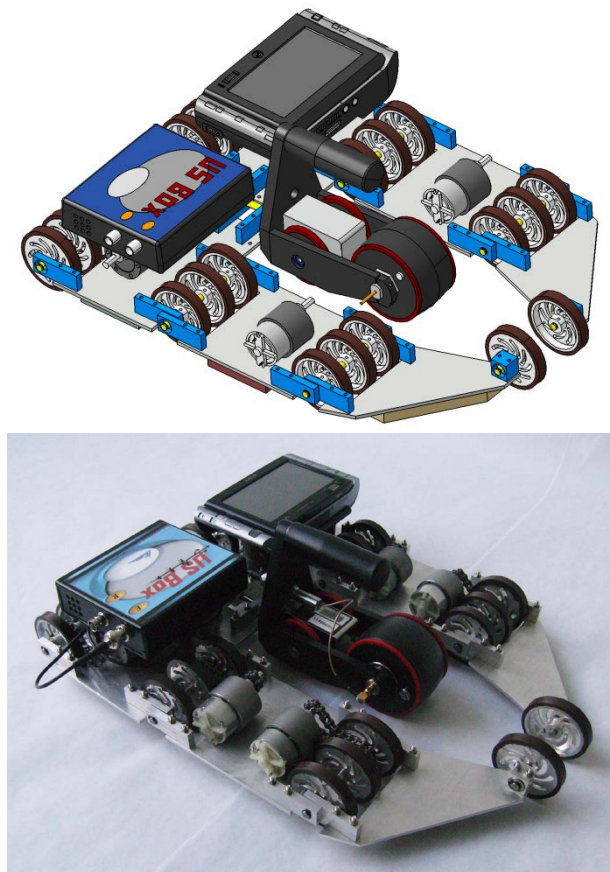


Figure 1: Design and prototype of the wall climbing robot for ultrasound NDT

The three section design not only enables the robot to transfer between sharp angled adjoining surfaces, but also improves its climbing ability on curvatures. Figure 2 shows the robot travelling around the pipeline surface both internally and externally and also when it is travelling along the pipeline. With a given overall size of the robot, when the robot is working on concave surfaces, the air gap between the magnets and surface in the sections design is much bigger than in the convex surface i.e. $d_1 > d_2$. As a consequence, the adhesion force on convex surfaces is greatly increased because of the reduction of the air gap. The main requirement is to keep the NDT probe in permanent contact with the surface at all times i.e. on concave and convex surfaces

and when moving across and along any pipeline. This design satisfies this requirement. The robot moves at a constant speed to scan for weld defects and corrosion. The robot speed can be modified by the operator to suit the inspection requirements. It has very good payload to weight ratio when climbing vertically, being able to carry nearly 8 kg extra payload in addition to its own weight of 5 kg. It is a high power wheeled design robot with capability to travel over any weld obstacle and provide the option to make angular transitions between surfaces of 0 to 60°. It is designed in three sections with the advantage of obtaining high pulling force in a low speed in any orientation on the surface, good manoeuvrability in both flat and curved surfaces. [7, 8]

It is driven by four powerful 15V DC motors with an output torque of 1000Ncm on each motor. They transmit the power to each set of wheels by connecting them with a steel chain, providing a big pulling force and highly secure transmission.

It is driven by four powerful 15V DC motors with an output torque of 1000Ncm on each motor. They transmit the power to each set of wheels by connecting them with a steel chain, providing a big pulling force and highly secure transmission.

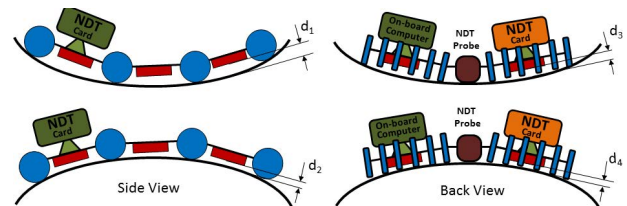


Figure 2: Adaptation to surface curvatures

3. MECHANICAL DESIGN OPTIMIZATION

Static and dynamic force analyses are necessary to evaluate and develop the optimum design parameters. In this section, Static and dynamic force analysis for the wall climbing robot is carried out.

3.1 Static Analysis

The stability of the wall climbing robot depends mainly on sliding failure, fall over failure or turn over failure as shown in figure 3. Static analysis helps to find the design parameters to address these stability concerns.

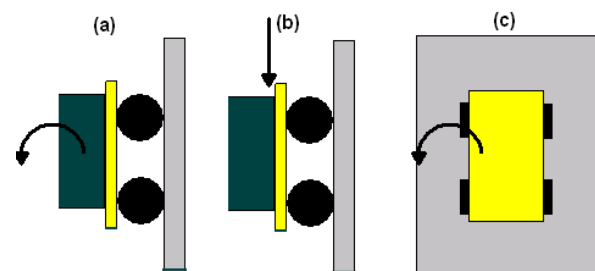


Figure 3: Stability factors a) turn-over failure; b) sliding failure, c) roll over failure

3.2 Sliding Avoidance

The ideal wall climbing robot should do climbing surface transitions and climb on surfaces with different slopes. To understand the forces acting on a robot, consider the forces acting on a robot resting on an inclined plane as shown in figure 4. The slope of the inclined plane is “ θ ”.

W = weight of the robot

θ = angle of inclination

F_m = magnetic adhesion force

μ = coefficient of friction of wheels

d = distance of centre of gravity from the climbing surface

L = distance between front and rear wheels

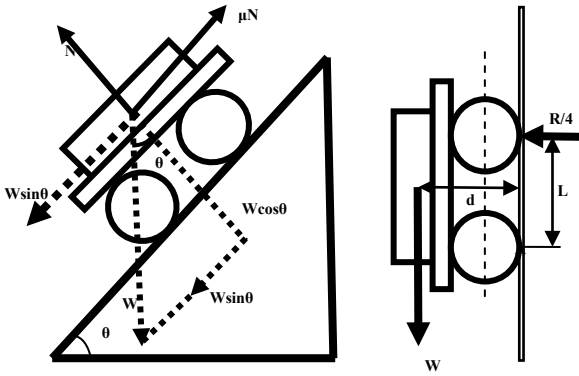


Figure 4: free body diagram of robot moving on an inclined plane

$$\sum F_y = W \cos \theta + F_m - N = 0$$

$$N = W \cos \theta + F_m$$

$$\sum F_x = W \sin \theta - \mu N$$

or

$$N = \frac{W \sin \theta}{\mu}$$

$$W \cos \theta + F_m = \frac{W \sin \theta}{\mu}$$

$$F_m = \frac{W \sin \theta}{\mu} - W \cos \theta$$

For the robot to avoid slipping

$$F_m > \frac{W \sin \theta}{\mu} - W \cos \theta$$

For the special case of wall climbing robot moving on a vertical surface

$$\theta = 90$$

$$F_m > \frac{W}{\mu} \quad (1)$$

In order to avoid sliding/slipping of the robot, the magnetic adhesion force should be greater than $\frac{W}{\mu}$. The stability of the robot can be increased by either increasing the coefficient of friction of wheel tyre or decreasing the robot weight.

3.3 Turn-over Avoidance

From Figure , Taking moment about point A,

$$\sum M = W \times d + \frac{R}{2} \times L = 0$$

$$R = -\frac{2W \times d}{L}$$

$$F_m = R$$

$$F_m = -\frac{W \times d}{2L}$$

To avoid Turn over, the adhesion force should satisfy equation 2.

$$F_m > \frac{W \times d}{2L} \quad (2)$$

For a given adhesion force, equation 2 can be satisfied by minimising the ratio $\frac{d}{L}$. This means that the centre of gravity should be as close to the surface as possible and the distance between the wheels should be large. Equation (2) shows that in order to avoid turnover, the robot centre of gravity should be kept as low as possible.

The stability criteria to avoid sliding and turn over:

$$F_m > \max \left\{ \frac{W}{\mu}, \frac{W \times d}{2L} \right\} \quad (3)$$

4. ADHESION FORCE

4.1 Magnetic Adhesion

The wall climbing robot uses magnetic adhesion force. Arrays of permanent magnets are split into three modules of the robot, called back, middle and front magnetic blocks, see figure 5. The magnets are attached to the bottom of three main flux concentrator plates in each half side of the robot. The adhesion force has been calculated for all three blocks independently by using finite element magnetostatic analysis.

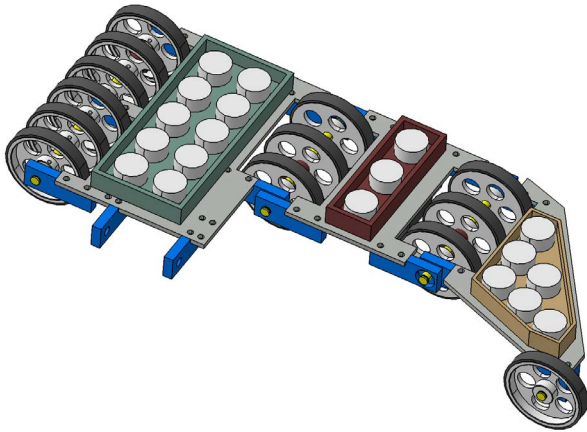


Figure 5: Half section of robot showing the three blocks of permanent magnets – Bottom view

The largest block of ten magnets (shown in figure 5 and figure 6) was first modelled in ANSYS design modeller and then imported into ANSYS Magnetostatic analysis. Like all the Finite element methods procedure, the meshing of the magnets was carried out and the boundary conditions were defined and simulated. The results of the simulations were verified by experimental results to validate the simulation setup and boundary conditions.

4.2 Adhesion Force Analysis

The ANSYS Magnetostatic Analysis is able to analyse different magnetic properties of the blocks. It includes flux density, field intensity, force simulation, torque, energy and magnetic flux. The same arrangement of blocks of permanent magnets are placed on both sides of the robot, but for the ANSYS analysis we have evaluated just one side, so the total adhesion forces available are double the forces shown in the table 1. [4]

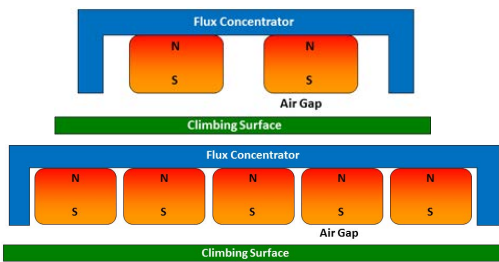


Figure 6: Arrangement of block magnets - side and long view

Figure 6 shows a conceptual design of the biggest magnetic block. It is placed in the back of the robot where the highest attraction force is required in the robot. It is composed of a magnetic flux concentrator with 5mm thick mild steel, two groups of neodymium magnets N35 with 20 mm diameter and 10 mm height (ten in total) and minimum technical requirement of 5 mm air gap between climbing surface (usually steel) and the magnets.

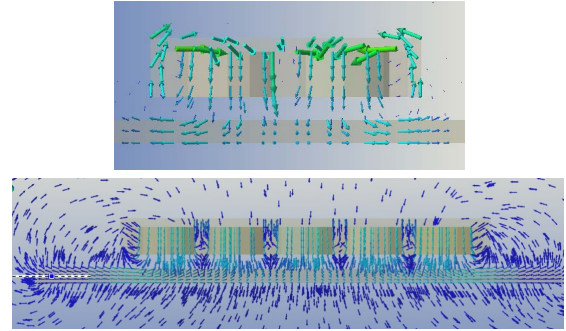


Figure 7: Magnetic flux line analysis for each block model.

The figure 7 is showing the flux lines around the block, the north poles of two magnets by side view are facing the flux concentrator. The magnetic lines of force travel from its north pole into the flux concentrator. To complete the magnetic circuit, these flux lines cross into the south pole after passing through the wall as shown. The front view where the five magnets are placed is clear the picture where the attractions force is strongly acting over the surface.

Table 1: Effect of Air gap on adhesion force (at wall thickness of 5mm)

Air Gap (mm)	Adhesion force (N)		
	Front Magnetic circuit	Middle Magnetic circuit	Back Magnetic Circuit
1	768.0268	416.2827	1424.503
2	417.8724	227.8784	804.2417
3	265.6434	138.386	511.5625
4	181.6449	89.88333	346.3584
5	132.4253	59.10403	248.3117
6	98.66827	41.24354	184.4507
7	79.34253	31.17378	145.6585
8	62.88417	23.2141	117.8043
9	50.37921	17.20698	96.96271
10	41.02408	13.19677	79.66313

Table 1 shows the adhesion force due to different magnet block arrangements of the robot. These magnetic arrangements include the concentrator plate, variable air gap between the magnets and the climbing surface and a 5 mm thickness of the wall. Our wall climbing robot has a constant air gap of 5mm; obviously, if the air gap is smaller, then higher adhesion forces can be obtained.

Effect of Air gap on adhesion force (at wall thickness of 5mm)

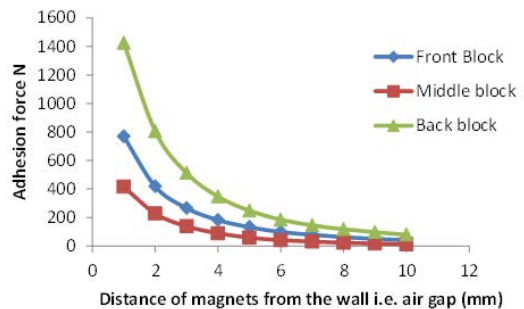


Figure 8: Results of ANSYS Magnetostatic Analysis

Figure 8 shows the air gap refers to the distance between the face of the magnet and the wall. If the air gap is increased, the magnetic adhesion decreases, but this air gap is necessary to avoid obstacles. Furthermore, when the thickness of the wall is increased from 0.1mm to 1mm, the adhesion force increases gradually. At 1 mm, the magnetic flux is almost maximum. Any further increase in wall thickness does not have considerable effect on the adhesion force. And finally, the geometry and construction material (e.g. relative permeability) of the concentration plate plays an important role in optimizing the adhesion force. [1, 4]

5. ROBOT CONTROL

The robot on-board controllers include two motor control modules, small computer system and one NDT card with ultrasound NDT probe. All cards are connected to the computer via USB and the on-board computer is connected to the ground via an Ethernet interface; so that, the operator can control the robot and the NDT devices via Ethernet network. All the on-board modules with standard USB interface are plugged to a USB hub and then connected with the computer.

The NDT application and graphic user interface (GUI) are placed on-board, this guarantees that all information is safe and the operator does not need to be worry about losing connection or interference from other devices.

The operator can access the on-board computer via Wi-Fi wireless communication to just supervise the inspection or to control the robot manually. Furthermore, all the on-board devices are powered by a high capacity lithium-ion Polymer (Li-Po) battery pack, so that the robot is totally umbilical free. See figure 9 for a schematic of the control system.

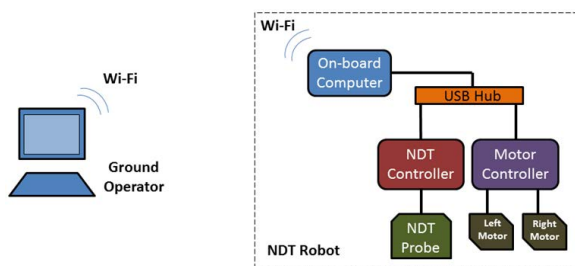


Figure 9: Schematic diagram of the Control System - NDT robot

6. NDT ULTRASOUND

The robot carries a single wheel probe to test weld defects, thickness or corrosion. The single element wheel probe is provided by Sonatest Ltd. It uses rubber technology for near-dry Ultrasonic coupling. The probe is designed to operate between 1MHz and 10MHz and is able to run in a low pressure tyre of 58mm diameter. It can be operated with or without an optical position

encoder, placed in the back of the wheel probe.

The NDT ultrasonic card, US.BOX of Lecoer electronique, collects data either in A scan mode or in Remanent mode. The A scan mode has the possibility to detect the presence of a defect, to determine its position and to evaluate its reflection capacity. The signal is digitized at 80MHz on the time base, and is represented by 1000 samples. Moreover, a peaks capture system allows the measurement of the amplitudes with a precision equivalent to sampling at very high frequency. The Remanent mode gives priority to posting, in order to be able to carry out a visual monitoring at recurrence frequencies incompatible with our visual capacities. In other words, Remanent visualization displays only one sequence every N samples, the other samples are not lost, the software only posts the best one (greatest echoes seen during the acquisition).

The NDT card interface is USB 2.0 at speeds up to 480 Mbps. The USB cable links without external power supply. The Transmitter generates 230 Volts (1 volt step) square pulses with width adjustable from 25 nS to 2 μS, wave train option, 100 Hz to 20 KHz. The Receiver Gain is 100 dB (0.1 dB step), DAC curve 80 dB, Filters 1 MHz to 10 MHz and one broadband, reflexion / transmission mode, Bandwidth 0.5 MHz to 25 MHz. The Analogue to digital converter is 12 Bits 160 MHz.

7. NDT RESULTS

The project had achieved some manual NDT test with the purpose of understand some pre-defined defects in different conditions like depth, size and shape. The NDT board used was the US-BOX of Lecoer electronique with a wheel probe ultrasonic sensor of Isotest Company. The results are presented considering visible pre-defined defects of three different test pieces of 50x50x200mm size; on this document only test piece 1 are presented.

The trials were carry out with manual NDT inspection over the mock-ups to analyse the different types of defects, as a results, the NDT ultrasonic sensor identify them as expecting.

The figure 10 is showing the test piece 1; this mock-up has five transversal cuts of different size in a constant distance between them. It is simulated a weld defect behind the wall.

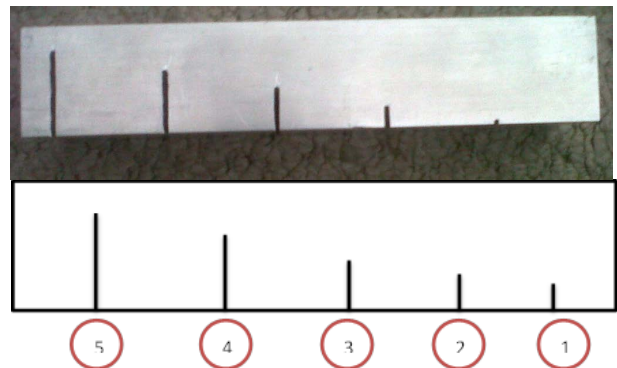


Figure 10: Test piece 1 with transversal cuts, simulated weld defects

The result of manual evaluation has a clear picture of how the ultrasonic responds on each pre-defined defect, where, doing a comparison between the five graphs, it is possible to observe how the signal get bigger on the first cut, and it begins to become smaller until the last defect. See figure 11.

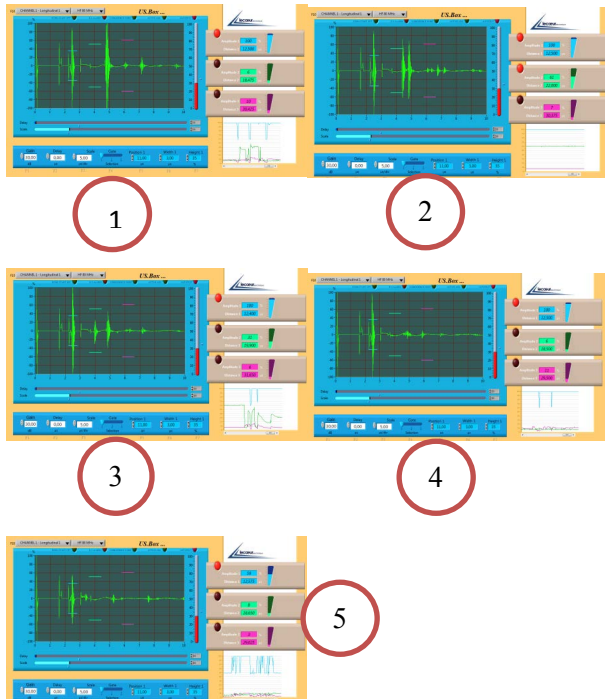


Figure 11: Result of analysis in test piece 1.

CONCLUSIONS

The lightweight NDT robot has been designed with the capability of climbing on steel walls carrying a payload of up to 8 kg. The high payload capability, considering the small size of the robot, has been obtained by using rare earth magnets, magnetic flux concentrators to increase adhesion forces and a mechanical design that keeps the magnet arrays at a more or less constant distance from the surface even when moving on large surface curvatures. It is able to climb on curved surfaces with excellent manoeuvrability, and can transfer between angled surfaces.

The robot uses ultrasound NDT to detect weld defects, thickness of the steel wall and surface corrosion

FUTURE WORK

The main focus will be on investigating other arrangements of the permanent magnets so that a uniform field can be generated between two axles of the robot.

Validate the automated ultrasound NDT trials with traditional manual inspection.

REFERENCES

- [1] Shang J., Bridge B., Sattar T.P., Mondal S. and Brenner A., "Development of a Climbing Robot for Weld Inspection", *Proceedings of the 10th International Conference on Climbing and Walking Robots and Supporting Technologies for Mobile Machines, CLAWAR 2007*, Singapore, 2007.
- [2] Bridge, B., Sattar T.P., Leon H., "Climbing Robot Cell For Fast And Flexible Manufacture Of Large Scale Structures", *22nd International Conference, CAD/CAM Robotics and Factories of the Future (CARS & FOF 2006)*, pp 584-597, Eds Narayanan, Gokul Kumar, Janardhan Reddy, Kuppan, ISBN Narosa Publishing House, ISBN 13:978-81-7319-792-5, ISBN; 10:81-7319-792-X, 19-22 July 2006.
- [3] Sattar T.P., Zhao Z., Feng J., Bridge B., Mondal S., Chen S., "Internal In-service Inspection of the floor and walls of Oil, Petroleum and Chemical Storage Tanks with a Mobile Robot", *5th International Conference on Climbing and Walking Robots and the Support Technologies for Mobile Machines*, pp 947-954, Edited by Philippe Bidaud and Faiz Ben Amar, ISBN 1 86058 380 6, Professional Engineering Publishing Ltd. UK, 2002.
- [4] Hussain S., Sattar T. Salinas E. Parameters Analysis and Design Framework for Magnetic Adhesion wall Climbing Wheeled Robot, *International Journal of intelligent System and applications*, 2012, to be published.
- [5] Sattar Tariq P., Leon-Rodriguez Hernando Efrain, Jianzhong Shang, "Amphibious NDT Robots", *Climbing and Walking Robots, Towards New Applications, International Journal of Advanced Robotics Systems*, Chapter 6, 24 pages, ISBN 978-3-902613-16-5, 2007.
- [6] Shang, Jianzhong; Sattar, Tariq; Chen Shuwo; Bridge Bryan, "Design of a Climbing Robot for Inspecting Aircraft Wings and Fuselage", *Industrial Robot: An International Journal*, vol. 34, No. 6, 2007, Emerald Group Publishing Limited, ISSN 0143-991X, 2008.
- [7] Fernández R, González E, Feliú V, González A., A Wall Climbing Robot for Tank Inspection. An Autonomous Prototype, *36th Annual Conference on IEEE Industrial Electronics Society*, pages 1424 – 1429, ISSN: 1553-572X, 2010.
- [8] F. Tâche, W. Fischer, G. Caprari, R. Siegwart, R. Moser, and F. Mondada, "Magnebike: A magnetic wheeled robot with high mobility for inspecting complex-shaped structures," *Journal of Field Robotics*, vol. 26, pp. 453-476, 2009.